PROCESSING and ACCURACY summary: GERB L2 Edition 1

GERB project team, last update January 2018

Collated by J E Russell

Please cite: Harries et al. 2005 when referencing GERB data.

Contents

Definition of terms

Level 1.5 data – GERB Non-Averaged, Non-Rectified, Geolocated products. Calibrated filtered radiances as observed. See level 1.5 user guide for further detail

SEVIRI – Spinning Enhanced Visible and Infrared Imager. A meteorological imager on each of the Meteosat Second Generation satellites which observes the Earth in 11 narrow-band spectral channels every 15 minutes with a sub-satellite sampling distance of 3km.

SW and TOT – abbreviations used to denote respectively the shortwave and total channels of the GERB radiometer including the weighting of the spectral response.

LW – abbreviation used to denote the synthetic longwave channel, created by the weighted subtraction of the SW from the TOT. It includes the spectral weighting of the synthetic channel response.

RSW and OLR – abbreviations for Reflected Shortwave and Outgoing Longwave Radiation, used to explicitly denote the reflected solar and emitted thermal radiation streams respectively.

GERB-like – estimates of the broad band RSW and OLR obtained from SEVIRI averaged up to the temporal and spatial scale of one of the GERB products.

PSF – Point Spread Function. Describes the spatial variation in the weighting of the GERB pixel footprint.

1. GERB data processing

This is a brief description of the standard processing to GERB level 2 products from the GERB level 1.5 calibrated, irregularly gridded SW and TOT channel filtered radiances. For a description of the GERB instrument see Harries et al. 2005. Further details of the processing are included in Dewitte et al 2008, Clearbaux et al 2008a and 2008b,

The GERB level 1.5 filtered radiances are derived directly from the GERB observations without employing SEVIRI data in the processing, however their geolocation is determined via matching to SEVIRI observations which is included in this description. Further use of SEVIRI data is made in several capacities in processing the level 1.5 to 2 products.

Background detail on the level 1.5 product production is contained in the level 1.5 userguide.

The processing steps can be summarised as:

- The level 1.5 data are first geolocated and a synthetic LW channel measurement derived by a weighted subtraction of the SW from the TOT.
- Spectral correction of the SW and synthetic LW filtered radiances is performed to derive the incident RSW and OLR radiances.
- The influence of the non-uniform PSF of each pixel is considered and a correction for its effect made for some of the GERB level 2 products. Finally, a real-time scene identification is performed to enable fluxes to be estimated.

Geolocation

Errors in the GERB geolocation not only affect the interpretation of the resulting products, but also influence the accuracy of the GERB processing, as it relies on accurate matching to SEVIRI to enable SEVIRI derived parameters to be related to the GERB observations. The GERB SEVIRI matching accuracy demands GERB geolocation accuracy better than around one tenth of a GERB pixel, which requires knowledge of the GERB pointing to within 0.4 arcminutes. This is extremely difficult to achieve on a spinning satellite. Noise in the satellite spin information and instrument pointing; distortions to the GERB optics due to the 16 g accelerations experienced by the instrument as a consequence of its location on the edge of the spinning satellite, and unknown details of the misalignment between structural and satellite spin axes coupled with the evolution of all of these with time, contribute to the problem.

For these reasons an empirical solution to the GERB geolocation is employed. SEVIRI images are geolocated at EUMETSAT by matching each scan line to landmarks (e.g. coastlines), and the GERB geolocation is defined by matching GERB observations to these geolocated SEVIRI data.

To enable this, a “GERB-like” broadband estimate is derived from the SEVIRI narrow-band data as described in the next section. For each GERB scan the difference between the SEVIRI estimated and GERB observed radiances is minimised by varying a range of parameters which relate to the orbital, optical and acquisition time details that determine the GERB pointing. Persistent biases between the GERB and SEVIRI geolocations should be minimised by this approach, although the absolute accuracy will depend on the accuracy of the SEVIRI geolocation and the matching itself will be subject to statistical noise.

Unfiltering

The GERB channel observations, L_{obs}^{SW} and L_{obs}^{TOT} are the result of the incident OLR and RSW spatially convolved with the pixel PSF and spectrally weighted by the GERB broadband SW

or TOT channel spectral response. The response of the TOT channel covers both the RSW and OLR spectral domains. The SW channel is simply the TOT channel plus a quartz filter. Its spectral range is primarily limited to the RSW, but does contain a small contribution from the OLR that is present in the spectral range of the SW channel. Unfiltering these observations describes the entire process of deriving the separate incident radiation streams from the channel responses. It is broken down into three distinct steps: separation of the LW from the TOT, spectral correction and spatial normalisation.

After geolocation the GERB TOT observations are linearly interpolated in time and space to the SW observation time and location. A synthetic LW observation is produced from a weighted subtraction of the SW from the TOT. The weighting accounts for the mean effect of the quartz filter, $\bar{T}$, defined for a reference scene as part of the ground calibration.

Regressions on a combination of simulated spectra and an observational dataset of matched broadband and SEVIRI measurements are used to derive narrow band to broadband relationships. The relations are applied to the SEVIRI radiances, averaged over 3x3 SEVIRI pixels, to produce broadband estimates at the so-called 'GERB HR' pixel scale. These are used to geolocate the GERB data, enable spectral correction and inform on the spatial variation of the scene within the GERB footprint.

The broadband components to be determined are the incident broadband OLR and RSW arriving at the instrument:

$$L_{scene}^{RSW} = \int_{\lambda=0}^{\lambda=\infty} L_{obs}^{RSW}(\lambda)d\lambda \qquad [1]$$

$$L_{scene}^{OLR} = \int_{\lambda=0}^{\lambda=\infty} L_{obs}^{OLR}(\lambda)d\lambda \qquad [2]$$

where $L_{obs}^{RSW}(\lambda)$ and $L_{obs}^{OLR}(\lambda)$ are respectively the spectral distribution of the RSW and OLR radiance in the direction of the GERB instrument from a given scene.

Their spectrally filtered counterparts are given by:

$$L_{RSW,scene}^{sw} = \int_{\lambda=0}^{\lambda=\infty} r_{GERB}^{sw}(\lambda)L^{RSW}(\lambda)d\lambda \qquad [3]$$

$$L_{OLR,scene}^{sw} = \int_{\lambda=0}^{\lambda=\infty} r_{GERB}^{sw}(\lambda)L^{OLR}(\lambda)d\lambda \qquad [4]$$

$$L_{OLR,scene}^{lw} = \int_{\lambda=0}^{\lambda=\infty} r_{GERB}^{lw}(\lambda)L^{OLR}(\lambda)d\lambda \qquad [5]$$

$$L_{RSW,scene}^{lw} = \int_{\lambda=0}^{\lambda=\infty} r_{GERB}^{lw}(\lambda)L^{RSW}(\lambda)d\lambda \qquad [6]$$

where the SW and synthetic LW channel spectral responses $r_{GERB}^{sw}(\lambda)$ and $r_{GERB}^{lw}(\lambda)$ are related to the ground measurements of the total channel response $r_{GERB}^{tot}(\lambda)$ and quartz filter transmission $T_{quartz}(\lambda)$ and the average quartz filter value, $\bar{T}$ used to derive the synthetic LW channel as follows:

$$r_{GERB}^{sw}(\lambda) = T_{quartz}(\lambda)r_{GERB}^{tot}(\lambda) \qquad [7]$$

$$r_{GERB}^{lw}(\lambda) = T_{quartz}(\lambda)r_{GERB}^{tot}(\lambda) - \frac{T_{quartz}(\lambda)}{\bar{T}}r_{GERB}^{tot}(\lambda) \qquad [8]$$

To determine the spectral correction factor for each GERB observation, the HR broadband estimates are interpolated to the GERB observation time and convolved with the PSF of the GERB pixel. The correction is then given by the ratio of the estimated OLR or RSW to their

spectrally filtered LW and SW channel counterparts. This correction, applied as a multiplier to each GERB radiance observation, accounts for the effect on that specific scene of the structure in the channel spectral response. It removes the small amount of OLR present in the SW channel which is added to the synthetic LW. It also adjusts for any difference between the mean effect of the quartz filter for the actual observed scene and the reference scene used to define the average filter transmission employed in the generation of the LW radiance. As the structure in the GERB spectral response is broad and smooth, and the correction is given by the ratio of two SEVIRI derived quantities, many biases in the contributing terms will cancel, greatly reducing the effect of their inaccuracies on the spectral correction.

To produce the ARG level 2 RSW and OLR radiances, the spectrally corrected radiances associated with three consecutive SW-TOT scan pairs, are interpolated to a regular grid and averaged. These ARG radiances are subject to the effect of the non-uniform spatial averaging of the GERB footprint. This effect is corrected in the other GERB level 2 products using the spatial detail contained in the HR broadband estimates, and information provided by the overlap between the PSFs of adjacent GERB pixels as described in the following paragraph.

The individual SEVIRI based broadband radiance estimates are iteratively corrected, until the ratio at the GERB footprint scale between the adjusted SEVIRI estimates and the GERB observation varies smoothly across adjacent observations. In essence, this exploits the overlap between the PSF of adjacent GERB pixels to improve the fidelity of the higher resolution partitioning of the footprint signal, and ensures consistency across GERB footprints of the higher spatial resolution information. The resulting corrected broadband estimates are then normalised and their relative variation used, along with knowledge of the GERB PSF, to apportion the GERB footprint observations to the HR scale. The apportioned radiances are corrected for the PSF weighting according to their location and interpolated to the SEVIRI acquisition time.

The result is presented to users in the GERB level 2 HR product to enable the production of custom regional averages for the purpose of re-gridding for model comparison or comparison with other instruments. They are also provided pre-averaged over exact 15 minute time slots and to a spatial scale similar to the GERB sampling distance in the GERB level 2 BARG product.

Implicit in the spatial correction is the assumption of large scale coherence of the observed scene. This assumption breaks down if the GERB footprint boundaries are aligned with strong scene boundaries such as coastlines. In these cases, instead of providing improvement in the accuracy of the spatial partitioning of the observation, the correction process results in some smearing of the higher resolution spatial information and apparent loss of spatial resolution. However in all cases the consistency it provides across GERB pixels ensures the noise introduced by this step will cancel to the same extent when averaging the result, irrespective of whether the averaging is aligned with the original GERB pixel sampling. This ensures that both the BARG product radiances and appropriate custom averages produced from the HR product have similar accuracies and that these are in general commensurate with the GERB footprint level accuracy. One caveat is that this will not be the case if averaging attempts to exploit the higher spatial presentation of the HR radiances by selecting points to average based on properties at the HR scale. In this case noise is not likely to cancel to the same extent in the averages and higher errors should be expected.

Flux Retrieval

Whilst the GERB instrument responds to the incident broadband radiance, it is the broadband top of the atmosphere flux that is the quantity required for most applications. This flux is the angular integration of the radiance in azimuth and elevation over the upper

hemisphere (see figure 1). To determine its value from the observed directional radiances requires the angular distribution of the radiation field for that scene to be known. This information can be derived from statistical analysis of multi-angle observations of a wide range of scenes or determined with the aid of simulations. In either case the conversion from radiance to flux will depend on the scene, the viewing geometry and also, in the case of the solar flux, the incident angle of the solar beam. Both approaches are expected to result in some statistical noise in the derived fluxes.

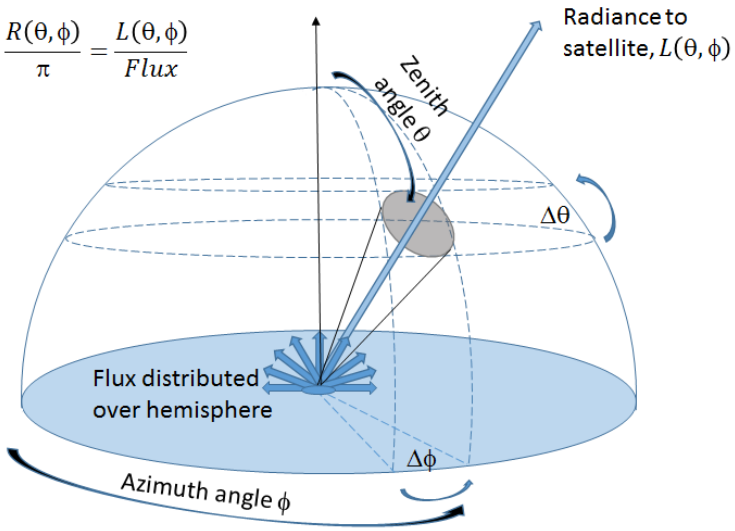

Figure 1. Relationship between observed radiance and flux, illustration azimuth and zenith angle definitions and anisotropy factor R.

As geostationary observations are obtained from a fixed viewing point, they pose particular challenges as viewing angle dependent noise in the radiance to flux conversion will not reduce with temporal averaging and must be considered a bias. Additionally, the accuracy of the instantaneous fluxes derived is sensitive to the detail lacking in the original scene classification used in creating the angular distribution models, and to what extent this averages out differences in the radiance distributions of the scenes within each class.

Solar fluxes:

The GERB reflected solar fluxes are derived from the radiances using angular distribution models which are primarily empirical. These have been built up from broadband observations obtained by the CERES instrument on the Tropical Rainfall Measuring Mission (TRMM) with some supplementary modelling used to fill in missing observational conditions (Loeb et al., 2003). The observational data is stratified into different scene types according to underlying surface, cloud cover, cloud optical depth and cloud phase. Diurnal symmetry is assumed, with broadband albedo provided as a function of solar zenith angle for each scene class. The fraction of energy in each angular viewing range for each solar zenith and class is then described by an anisotropy factor, *R*, which is a function of viewing zenith angle and the relative azimuth angle between the viewing vector and the solar beam. The GERB processing determines the scene and estimates the reflected solar flux at the HR pixel scale by multiplying the spatially reapportioned GERB reflected solar radiances by $\frac{\pi}{R'}$. Here *R'* is the anisotropy factor provided by the angular distribution model for the observed scene type, tri-linearly interpolated to the solar zenith angle, viewing zenith angle and relative azimuth angle of the GERB observation (see figure 1).

To assign a scene type to each GERB observation, a fixed surface type map is used and a SEVIRI pixel level, real time retrieval of cloud phase and optical depth employed (Ipe et al. 2007). The cloud phase determination uses the SEVIRI 10.8 μm channel with identified

cloud classified as ice when this brightness temperature is less than 255 K and as water otherwise. Cloud optical depth is retrieved for each SEVIRI pixel using either the 0.6 or 0.8 μm SEVIRI channel reflectance, depending on which offers the better cloud/clear contrast. In practice this means that the retrieval uses the 0.8 μm channel over ocean and the 0.6 μm over all other surfaces.

Cloud optical depth is determined from the difference between the observed and clear-sky reflectance scaled by the difference expected for a very thick cloud under the same conditions. Conversion from this scaled contrast to optical depth uses a function derived from simulations for the specific clear sky reflectance and observation geometry. The clear-sky reflectance used to choose the function and determine the scaled contrast is determined from 20 to 60 days of SEVIRI observations for that location at that time of day. For the operational processing, which is performed in near real time, only prior observations contribute to the clear-sky reference, but for reprocessing the reference period is centred on the current time. In both cases the number of days used varies with location in a predefined way, according to the expected cloudiness and seasonal variation of the clear-sky reflectance.

A threshold on the cloud optical depth classifies each SEVIRI pixel as clear or cloudy and this cloud mask is used to determine the cloud fraction at the HR pixel scale. The average over the classified cloudy pixel of the logarithm of the optical depth gives the associated HR cloud optical depth and the most prevalent phase defines the cloud as ice or water. In combination with the underlying surface map these parameters determine which angular distribution model is used to determine the reflected solar flux.

The fidelity of the reflected solar fluxes relies on the empirical angular distribution model applied being appropriate for the scene viewed. This requires that the GERB scene classification matches with the classification that would have been applied to CERES-TRMM observations. It also assumes that the angular distribution information derived from the CERES-TRMM observations captures the specific conditions of the GERB observations.

Thermal fluxes

The GERB emitted thermal fluxes are also determined at the HR pixel scale from the spatially apportioned GERB radiances on the basis of an anisotropy factor which is a function of viewing geometry and scene. In this case an understanding of the angular distribution of a given radiation field is gained from simulations, and scene classification is implicit as the anisotropy is determined directly from the observed SEVIRI narrow band radiances. Coefficients to enable the anisotropy factor to be determined from the SEVIRI 6.2 μm, 10.8 μm, 12 μm and 13.4 μm channel observations are derived for each viewing zenith angle range from regressions performed on a database of simulations. The longwave anisotropy is assumed to be a function of viewing zenith angle only: azimuthal variation is not considered and anisotropy effects on the emitted thermal of the solar illumination angle, due to differential heating for example, are ignored. This approach to deriving the thermal flux relies on the simulations accurately representing the angular distribution of energy of the scenes. Any errors in the modelled angular variation of radiance will result in viewing angle dependent errors in the derived flux, whilst deficiencies in the spectral variation of the scene may result in errors in the implicit classification of the scene and as a consequence an inappropriate radiance to flux conversion being applied. The basic concept behind the approach used is described in Clerbaux et al. (2003).

2. Filled data

For the ARG product for SZA 80 to 105° or within 15° of the ocean glint angle fluxes are missing. For the HR and BARG products special treatments are applied to *estimate* SW fluxes the resulting fill values are not intended to provide high instantaneous accuracy but to

enable low bias averages to be produced. Fill values are indicated by a flag in the product (see identifying filled points). Fill flux values include values where:

- The solar zenith angle is between 80 and 105°.
- The underlying surface is ocean and the radiance observation is obtained with a glint angle of <15°.
- The observation is identified as clear ocean and the radiance observation is obtained with a glint angle of <25°.

where the glint angle (ξ)+- is that at which specular reflection occurs over calm ocean and can be calculated based on the viewing and solar geometry as follows:

$$\xi = \cos\theta_0 \cos\theta + \sin\theta_0 \sin\theta \cos\phi$$

Where θ_0 is the solar zenith angle θ is the viewing zenith angle and ϕ is the relative azimuth angle. When the solar zenith angle is 80°-85° and for observations made over ocean within 15° of the glint angle, co-incident scene identification with SEVIRI is compromised. Filling uses scene identification for that location from earlier or later times. Filled SW fluxes are estimated based on the nearest in time valid cloud properties for that location as long as this is not more than three hours from the observation time (scene extrapolation).

For solar zenith angles between 85° and 105° twilight conditions, and for observations identified as clear ocean made within 25° of the glint angle, the observed radiation is not converted to flux but instead a climatological flux value is provided. In both these situations direct conversion of the radiance to flux using the TRMM ADMs is not reliable. For solar zenith angles between 85 and 105° considered as 'twilight' a fixed model based on the CERES empirical twilight model is used. This does not vary with location nor with the observed radiance. For observations over ocean identified as clear within 25° of the glint angle a monthly 'climatological' clear ocean flux based on the GERB observations for that location and the TRMM angular models is provided.

All fill values are provided to enable temporal averaging with low bias: instantaneous accuracy will be lower compared to the unfilled cases and the fill points are not intended to provide an accurate representation of the instantaneous flux. More detail on their uncertainty is provided below.

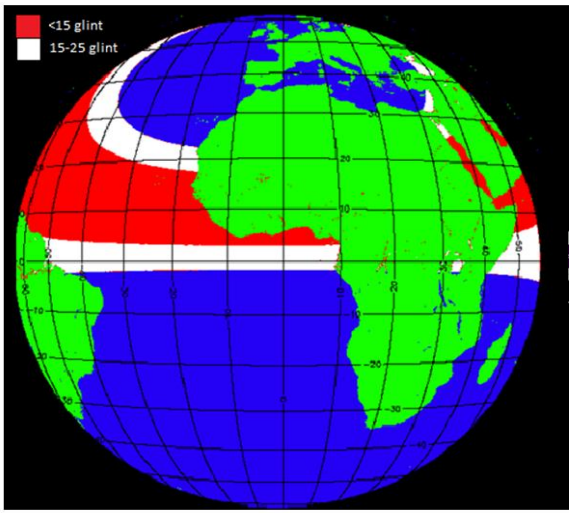

Figure 2. Example for June 2004 of ocean points which at some point in the day have glint angles < 15° (red) or in the range 15°-25° (white).

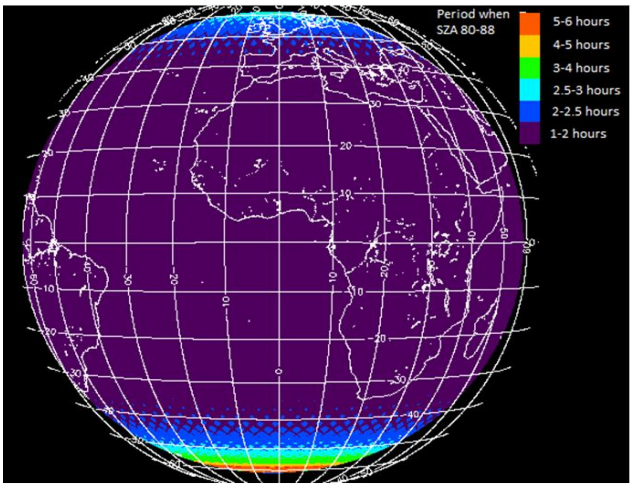

Figure 3. Example for June 2004 for the period of time each location is in the SZA range 80° to 88°

Figure 1 shows the locations where the surface is ocean and the glint angles reaches values less than 15° or 25° at some time of day for June. Figure 2 shows how many hours for an average day in June the solar zenith angle is the 80 to 88° angle range. The expected monthly mean error in SW fluxes when no filling is performed on the GERB data is shown in Figure 3, this is the difference between the average after filling and the average of just the unfilled points. By contrast the theoretical error in the monthly average when the filling procedures identified above are implemented is less than 1 W m^{-2} almost everywhere, only exceeding this values in a few places in the glint region.

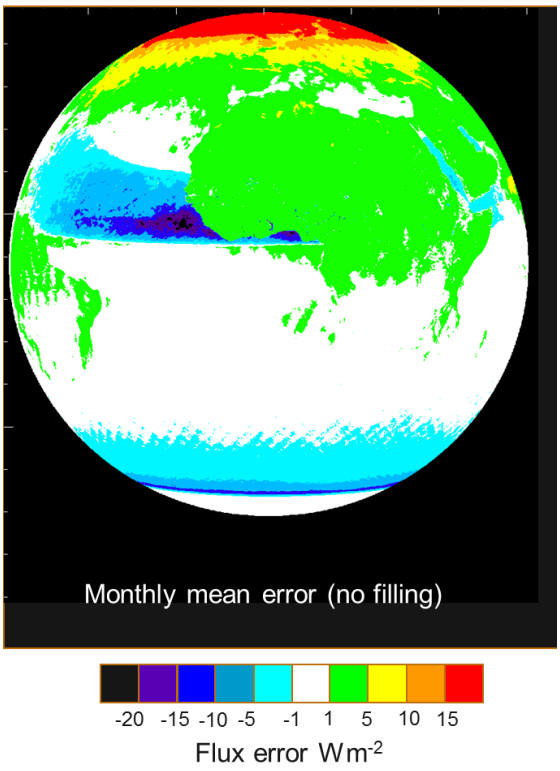

Figure 4. Expected error in the monthly mean if no filling is used (i.e. the missing data is filled with the average flux value). Example shown for GERB 2 June 2004

Identifying filled points

To identify points subject to filling by one of the methods above, a flag data set "status flag word 1" is included within the "rmib" group of the GERB HR? HDF file. The flag dataset is an

array with one point for each SW flux value. The flag value is determined at the HR product scale as a bit pattern where bit 0 set indicates the scene ID has been extrapolated, bit 1 set that a climatological ocean flux value has been used and bit 2 set that the flux value has been set according to the twilight model. In the BARG product flags from the contributing HR pixels are combined with a bitwise or, so the resultant flag in the BARG reflects all the filling types of the contributing HR pixels. In either case a flag value of zero indicates the SW flux has not been affected by any filling.

Decimal flag value	Bit pattern relation Bit 0: extrapolated scene Bit 1: ocean climatological flux Bit 2: twilight model	Meaning	Occurrence
0	000	No filling	Points not in twilight or glint conditions
1	001	Scene extrapolation	Twilight and glint conditions or other problematic cases where contemporaneous scene ID can't be made
2	010	Climatological ocean flux is used, no scene extrapolation	Outer glint region, where scene is not extrapolated, if scene identified as clear ocean
3	011	Scene extrapolation and climatological ocean flux is used	Inner glint region where scene determined by extrapolation is deemed to be clear ocean
4	100	Twilight model used	No scene extrapolation twilight model used

Table 1. Decimal values of the fill field, bit pattern and meaning for valid combination of bit flags in the HR product. Note in the BARG product due to combining flags from different contributing HR other bit pattern combinations are possible such as 5 however this would indicate twilight model was used in one part of the BARG gridpoint and scene extrapolation in other not that they occurred for the same point.

Twilight model

Twilight was defined by Rozenberg (1966) as the range of optical phenomena that occur in the atmosphere when the sun is approximately within 5°-10° of the horizon. For this range of SZA at the surface, the solar beam incident on clouds within the atmosphere both at that location and nearby becomes as or more important than solar energy incident at the surface. For SZA > 85° the standard TRMMS ADMs cannot provide a reliable conversion from radiance to flux based on the scene at that location and average SW fluxes based on global CERES observations (Kato and Loeb 2003) are used for the SZA range 85 to 105°. These twilight fluxes do not vary geographically or seasonally and thus provide no instantaneous information, they are provided purely to minimise the bias in averages that would exist if they were ignored.

Comparison between GERB 2 and CERES low sun observations and the CERES twilight model indicated that the CERES twilight fluxes could be used without any attempt to adjust for overall level difference between GERB and CERES calibration, however they are only

used for SZA up to 100° with all SW fluxes set to zero for SZA larger than this value. For GERB 2 they have in fact been adjusted to enable the GERB 2 calibration correction multiplier 0.976 to be applied, so strictly speaking should be multiplied by this number but not by any of the other adjustments such as the GERB 2 to GERB 1 or aging corrections. However, the 0.976 multiplier on these low flux values a small overall Wm^{-2} effect that is less than the bias in the monthly mean expected from the filling of the higher SZA so for simplicity it is recommended that all adjustments only be applied for the SZA up to 85° excluding the flagged twilight model points. This is detailed in the combined correction application explained in the quality summary.

Central value of SZA 1° range	Twilight model flux (W m^{-2})	Central value of SZA 1° range	Twilight model flux (W m^{-2})
84.5	48.3428	92.5	2.9716
85.5	39.7990	93.5	1.5336
86.5	31.7399	94.5	0.9251
87.5	24.9577	95.5	0.6051
88.5	18.4358	96.5	0.3768
89.5	12.4553	97.6	0.3004
90.5	7.5284	98.5	0.2401
91.5	5.0543	99.5	0.1802

Table 2. Baseline values of the CERES twilight model that are used in the GERB products. These values have been divided by 0.976 for the GERB 2 products to account for the calibration correction for this instrument.

Clear ocean climatology

Due to the large errors involved in converting to flux ocean radiances observed close to specular reflection, radiances for scenes identified as clear ocean observed at glint angles less than 25° are not used to estimate flux. In these cases the GERB monthly average clear ocean flux for that location, corrected to the solar geometry of the instantaneous observation is provided. The GERB monthly average clear ocean flux is determined from all ocean points by collecting near 'pristine' observations (no cloud or heavy dust aerosol in that HR or surrounding HR pixels[1]) which have glint angles > 25° and SZA < 80°. These are converted

[1] A pixel is included in the computation of the monthly clear-sky ocean adjustment factor if:

(1) sun glint angle >= 25
(2) solar zenith angle <= 70
(3) viewing zenith angle <= 70
(4) GERB cloud cover == 0
(5) (if MPEF cloud cover is available) MPEF infrared cloud cover == 0
(6) dust flag not set or undefined
(7) surrounded by 8 pixels meeting all of the above criteria
(8) (8) surface type is ocean

Condition (6) only excludes confirmed dust pixels and gives undefined dust pixels the benefit of doubt. Condition (8) is applied after condition (7) to ensure that ocean pixels right next to land pixels do not systematically drop out from the adjustment factor computation (provided that all other conditions are satisfied).

to albedo and corrected to the geometry of the observation to be filled using the TRMM angular models and then averaged. This is done for each location and will thus include both real variations and most location specific biases in the data. However, as any point which is identified as being contaminated by moderate-high dust loading is omitted from the average, biases associated with the radiance to flux conversion of dust contaminated points which other times of day may be subject to are not included in the climatology. Any bias introduced into the clear ocean flux due to cloud contaminated radiances being identified as clear will introduce a bias into the climatological value which is distinct to the original bias due to the correction for the solar geometry that is applied.

The climatological flux is best expressed as a ratio by which the TRMM model albedo is multiplied to match the GERB observations. This multiplier varies with location and is calculated for every ocean point for each month using all the pristine ocean observations which have glint angles > 25° and SZA < 80°. Figure 4 shows an example of the spatial and seasonal variation of the multiplier. Note the multiplier is only ever used for points that have glint angles < 25°. Thus the high ratio points off the Angola coast in June or off Guinea in November do not contribute to the products.

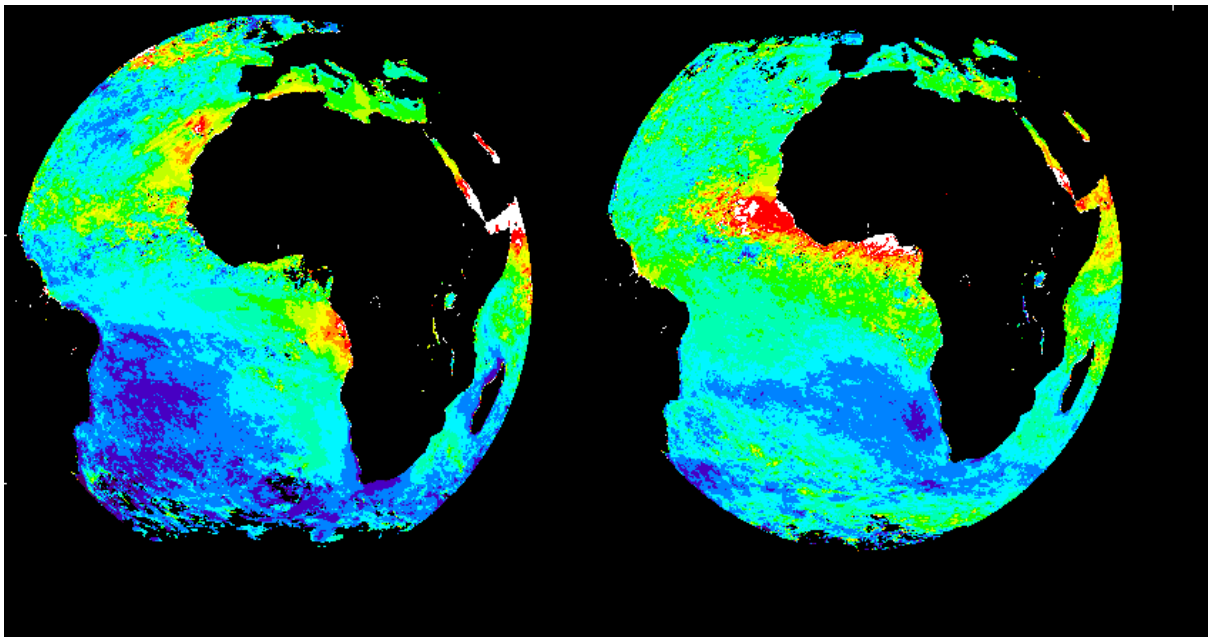

Figure 5. Ratio of the clear ocean climatology for June 2004 (left) and November 2004 (right). This ratio is derived from non-glint times of day and constitutes the average of the TRMM angular model divided by the GERB observations. (scale required)

The albedo for the glint region is thus the TRMM model adjusted to the GERB observations for that month. It is converted to flux by multiplying by the incoming solar for the glint conditions.[2]

---

[2] A bug in the GERB/TRMM adjustment factor calculation fails to consistently account for the annual variation in the Earth-sun distance in the incoming solar when converting the albedo to flux. The resulting error in the clear ocean fluxes reaches is up to 3.4% at the around the solstices, however as the clear ocean flux is small this is less than a couple of watts and thus small compared to other sources of errors such as cloud and aerosol contamination affecting the ocean ratio. Due to the limited occurrence of clear sky the effect is further diminished in averages that do not separate clear and cloudy conditions.

3. Processing and calibration uncertainty

Accuracy aims of the GERB products are 1% (of the typical full scale radiance) absolute accuracy of LW and SW radiances, and 0.1 GERB pixel absolute accuracy of the geolocation. The theoretical accuracy of the edition 1 GERB products does not meet all of these targets due to known issues which we plan to resolve in future releases. Below is a summary of our current understanding of the theoretical accuracy of the GERB radiances and geolocation.

Unfiltered radiances at launch uncertainty

The magnitude of systematic errors in the unfiltered radiances has been determined from the uncertainties provided for calibration sources and spectral response measurements. In addition the effect of un-flagged stray light and the theoretical accuracy of the SEVIRI inter-channel comparison are considered. Table 3 summarises the approximate magnitudes of these effects and determines an RMS combination of the contributions to derive an overall accuracy assessment of the unfiltered radiances. It should be noted that no random errors, including those that may be systematic for a particular scene type, are considered in table 3. Errors are quoted as a percentage where a fixed error in the quantities corresponds to a fixed fractional error in the unfiltered radiances, independent of the magnitude of the unfiltered radiances. Where a fixed error causes a fixed radiance error on the unfiltered radiances errors are quoted as a percentage of the typical full scale radiances which are taken to be 240 $Wm^{-2}sr^{-1}$ for the SW and 77 $Wm^{-2}sr^{-1}$ for the LW in correspondence with the accuracy requirements.

Error source	Reflected solar	Emitted thermal (night)	Emitted thermal (day)
Calibration sources absolute accuracy (1 SD uncertainty values)	~0.22%[3]	<0.05%[4]	
Calibration sources uniformity (full range over region used)	< 0.5%	Small	
Spectral response [5]	1.9% of typical full scale	<0.9% of typical full scale	<0.9% of typical full scale
Stray light (maximum effect in unflagged data)	<0.25 $Wm^{-2}sr^{-1}$ [6]		
	<0.1% of typical full scale	<0.3% of typical full scale	
Polarisation	<0.4%[7]	Small	
SEVIRI inter-channel calibration[8]	<1%	<0.1%	<0.1%
RMS combination of above errors	**2.25%**	**0.96%**	**0.96%**

Table 3. Estimates of the ground determined unfiltered radiance bias error sources and magnitudes.

[3] GERB 2 VISCS data implies errors on integrated quantities of between 0.13% (spectrally uncorrelated errors) and 1.08% (worst case spectrally correlated errors). As no separation of the spectrally correlated and uncorrelated errors are currently available for the GERB 2 VISCS calibration the value given above was determined from the GERB 3 VISCS calibration for which spectrally uncorrelated and spectrally correlated errors were provided separately.

[4] Linear sum of temperature probe calibration, drift and chamber radiation.

[5] Values indicate the largest effect over a wide variety of scene types. Uncertainty is determined as a linear sum of the effects of spectrally correlated and spectrally uncorrelated errors (1SD level) on the instrument spectral response.

We note that spot measurements on the flight spare detector obtained post launch with an improved measurement technique show a response that would lower the unfiltered shortwave radiances by approximately 3.5% across all scenes compared to the response currently in use. The difference may be due to a real variation between the in-obit and flight spare detector arrays; however an ongoing investigation is underway to determine if the difference indicates an unaccounted for systematic error in the original data.

[6] Error indicates the maximum impact of unidentified stray light. Data with stray light contamination between approximately 0.25 $Wm^{-2}sr^{-1}$ and 3.5 $Wm^{-2}sr^{-1}$ is processed to level 2, but flagged to indicate diffuse stray light contamination. Data with stray light contamination greater than ~ 3.5 $Wm^{-2}sr^{-1}$ is not processed to level 2 products.

[7] Worst case error for a completely linearly polarised source.

[8] Unfiltering the GERB radiances relies on SEVIRI observations. The effect on the GERB unfiltered radiances of the worst case SEVIRI inter-channel calibration error at a ±5% level is considered here. For SW a worst case effect is an overestimation of the unfiltering factor by 0.8% if the errors on SEVIRI 0.6μm is +5% and on 0.8μm and 1.6μm is −5%. For the longwave the worst case is found to be an overestimation of the unfiltering factor by 0.09% for −5% on 6.2μm, 7.3μm, 12μm and 13.4μm SEVIRI channels and +5% on 8.7μm and 10.8μm.

Random errors are considered in table 4. This table includes contributions from detector noise, interpolation and unfiltering. Uncertainties due to these sources are stated as percentages of the typical full scale radiances are before. The estimated 1SD random error in geolocation accuracy is stated in terms of GERB pixels. It should be noted that geolocation errors will lead to errors in the assigned filtered radiances for a given location, and additional errors due to a mismatch with SEVIRI in the unfiltering factor and the radiance to flux conversion factors. Whilst random in origin, unfiltering and geolocation errors can lead to systematic errors in radiances and fluxes ascribed to a particular scene type.

Error source	Reflected solar	Emitted thermal (night)	Emitted thermal (day)
Instrument noise	0.13% of typical full scale	0.4% of typical full scale	0.6% of typical full scale
Geolocation[9]		0.25 pixel	
Interpolation[10]	0.63% of typical full scale	1% of typical full scale	1% of typical full scale
Spectral overlap correction	0.02% of typical full scale	None	0.08%
Unfiltering	0.3% of typical full scale	0.05% of typical full scale	0.05% of typical full scale

Table 4. Estimates of the random errors on the unfiltered radiance.

Fluxes

GERB SW fluxes use the CERES TRMM ADMs for their radiance to flux conversion. Users are referred to the relevant CERES documentation and quality summaries for validation results details on the accuracy of the ADMs themselves (see Loeb et al. 2003).

Users should note that the implementation of the SW radiance to flux conversions for the Edition 1 GERB products is not identical to their application to the CERES data. CERES has different ADM versions derived from their TRMM, Terra and Aqua satellite instruments. GERB Edition 1 data uses the CERES TRMM ADMs. The CERES data used in the comparison studies shown in section 3 (edition 2b FM1 and FM2 data and edition 1b FM3 and FM4 data) use the Terra ADMs. GERB Edition 1 fluxes do not include an adjustment for the apparent aerosol optical depth and use interpolation of the monthly climatology to determine the wind speed for selection of the appropriate ocean ADM. In addition no interpolation for cloud optical depth and fraction is made. Comparison of co-angular fluxes between GERB and CERES indicates that these differences, in addition to differences in scene ID due for example to SEVIRI calibration bias, results in an average 1% offset between the GERB and CERES radiance to flux conversion factors. Thus all other differences aside, GERB fluxes are elevated by 1% compared to CERES for the same unfiltered radiance.

[9] Pixel error quoted is determined from the stability of the geolocation in the GERB 2 validation data set (V998) and represents approximately 1SD excluding the edge pixels.

[10] Errors quoted are 1SD for the maximum interpolation distance of 0.5 of a pixel, determined from high resolution scans over the central 100 columns of the Earth.

The ADMs which are the basis of the radiance to flux conversions are statistical in nature and thus a random error will be associated with the instantaneous flux estimates: the 1SD values of these errors are shown below. In addition SEVIRI measurements are used both for the scene identification used to choose the appropriate SW radiance to flux conversion factor, and in determining the longwave radiance to flux conversion. Thus, the effect of a 5% calibration error on the SEVIRI radiances and inter-channel calibration is also considered.

Error source	Reflected solar	Emitted thermal
SW ADM	~14 Wm^{-2} random error	
LW anisotropy		2.3% random error (of typical full scale)
SEVIRI channel calibration and inter-channel calibration[11]	< 0.5% bias < 2.3% random error (of typical full scale)	< 1.3% bias (of typical full scale)

Table 5. Addition error sources and approximate magnitudes to which the SW and LW fluxes are subject (see Loeb et al. 2003 for validation results on the CERES TRMM ADMs).

Bias errors in averages from fill points

Additional errors are expected in the flux for the filled points. As these are only intended to be used when making averages we consider only their effect on monthly average quantities, both the overall monthly average and the monthly timestep mean.

As the filled points occur at specific geometries they are systematic for a given time of day. That means that even after averaging over the month in the monthly time-step mean product there will be locations that are entirely composed of points filled using scene extrapolation. These points correspond to the locations that are experiencing glint or low sun conditions at this time of day. The locations will move with timestep and most locations will experience conditions requiring scene extrapolation for more than one time step. In the overall monthly mean the number of filled points contributing to the average will vary with location according the period of time in glint and under low sun conditions (see figures 2 and 3).

Scene Extrapolation Errors

As previously mentioned cloud properties cannot be retrieved under certain solar illumination conditions, i.e. SZA between 80 and 85° and within 15° of ocean glint angles for locations with an underlying 'ocean' surface (including inland lakes and rivers). In these cases a temporal nearest neighbour extrapolation is used with the closest in time retrieved cloud condition for that location assigned as long as the retrieval is within 3 hours of the observation[12]. The SW flux is then derived from the current radiance observed and the TRMM model for the extrapolated cloud conditions and the current solar geometry. For the filling within 15° of ocean glint the resulting instantaneous error can be very large, because whilst both ocean and cloud radiances are very bright at this geometry, these scenes have very different anisotropies. The scene assigned thus has a very large effect on the radiance to flux conversion and hence the final flux. Application of the cloud ADM in clear conditions in these cases leads to an overestimate of the flux which can be over 100Wm^{-2}, while

[11] Simulated effect on the derived fluxes of a 5% calibration error in the SEVIRI radiances used for scene identification in the SW. LW error determined as worst case effect of 5% inter-channel calibration errors in the LW on the determination of LW anisotropy factor.

[12] In cases where an earlier and later good retrieval are equally close in time to the point then the prior retrieval is used.

assuming a cloudy point is clear leads to a significant underestimate of the flux. However the overall bias averaged over consecutive days and or large regions is small.

To provide a theoretical estimate of the filling error and their characteristics we created “false glint” and “false twilight” conditions by looking at the same location at a different time of day when a contemporaneous scene ID was possible. The radiances at these different times were modified using the TRMM angular model associated with the identified scene to give the radiance that would be observed under the solar geometry conditions of the filled point. The effect of converting these modified radiances to flux based on a nearest temporal neighbour scene extrapolation of the type used for the fill point was then compared to the flux for the actual scene. The results are summarised in figures 6 to 10 below. These studies show that averaged over the full disk the bias in the monthly mean due to filling is < 0.2Wm^{-2}. The RMS error for the filled points is ~20Wm^{-2} for the instantaneous error and ~6Wm^{-2} for the monthly timestep mean.

As the need for filling and the sensitivity of the radiance to flux conversion to scene is solar and viewing geometry dependent, the amount of filled points as well as both the instantons and averaged errors vary with location, timestep and time of year. Figure 6 shows for July and November 2004 the average number of timesteps which experience extrapolation for that month and for the average error in the filled points at the monthly timestep scale.

The band affected by ocean glint angles < 15° can clearly be identified as having both a greater number of filled point than everywhere except the highest latitudes and experiencing the largest average filling error at the monthly timestep mean scale. All locations are affected by some filling during the period when the sun in the SZA range 80 and 85°, with the higher latitudes experiencing these conditions for longer. Absolute flux errors are smaller for the higher SZA filling due to the reduced solar illumination. However because of the timing in the day morning points will always use a later retrieval and evening points an earlier one, which will have some effect on the overall bias. An additional factor is the varying diurnal bias in the GERB cloud retrieval observed at large viewing zenith angles. At low sun this results in increasingly more cloud being detected with increasing SZA towards the edge of the Earth disc and makes the definition of the ‘true’ cloud amount in these locations and times somewhat ambiguous. Due to filling requiring a valid scene ID at the same location within 3 hours of the time filled some points remain unfilled. At very high latitudes in the winter hemisphere this results in not filling and no valid points. The hatching pattern that is present in the number of timesteps which experience filling and the average size of the filling error is a result of the temporal quantisation of the 15 minute HR products. This results in a corresponding quantisation in solar zenith angle change and hence number of filled points and filling error.

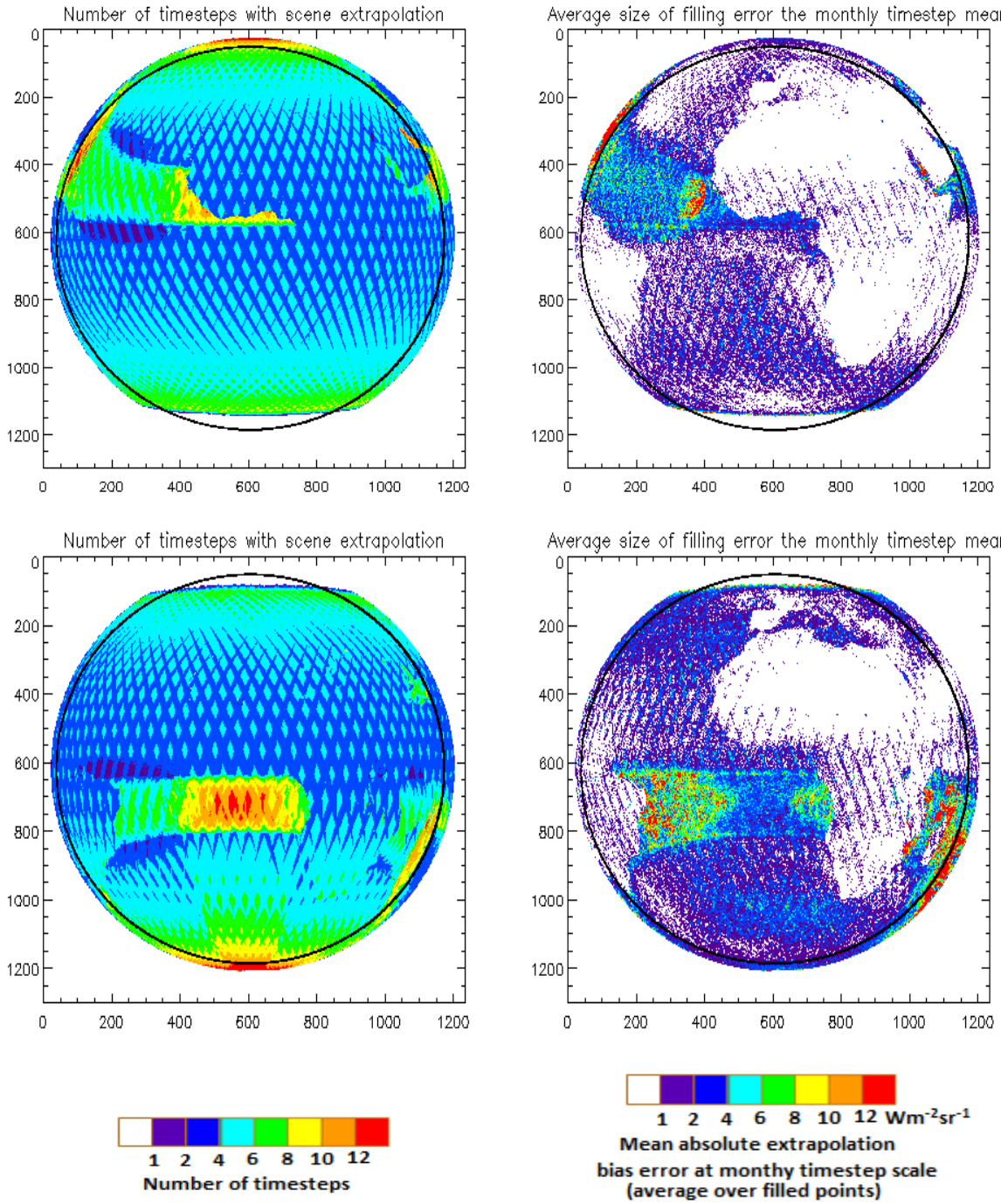

Figure 6. Number of 15' timesteps (left) for which scene extraplation is used due ot twilight or glint conditions for an average day. Estimated mean absolute bias error (right) in the extrapolated points at the monthly timestep scale. Top for GERB 2 July 2004, bottom for GERB2 November 2004. Black circle shows the limit of the 70° viewing zenith angle.

Figures 7 and 8 show the estimated error in the monthly timestep mean due to filling for some example timesteps calculated for the June and November 2004 data respectively. The band corresponds to the 80 to 85° low sun filling, the circle the <15° glint region for that timestep. As cancellation of scene misidentification errors varies with geometry so does the worst biases. Patterns of positive and negative bias can been seen in the glint region particularly in the November 2004 case shown in figure 8.

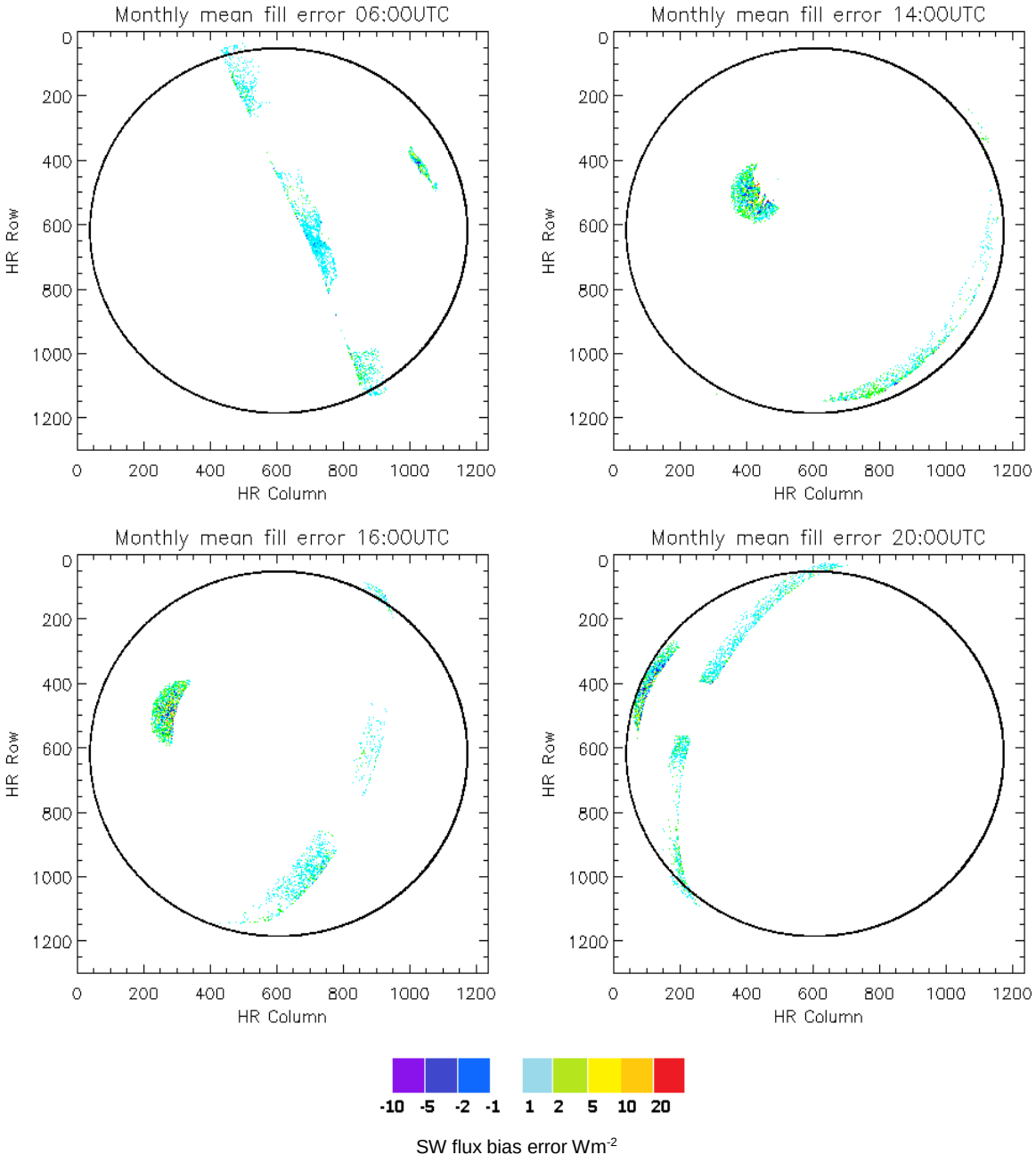

Figure 7: Theoretical bias error in the monthly time-step mean due to scene extrapolation. Above example calculated for GERB 2 July 2004 for the HR 1237x1237 grid point products. Black circle shows the limit of the 70° viewing zenith angle.

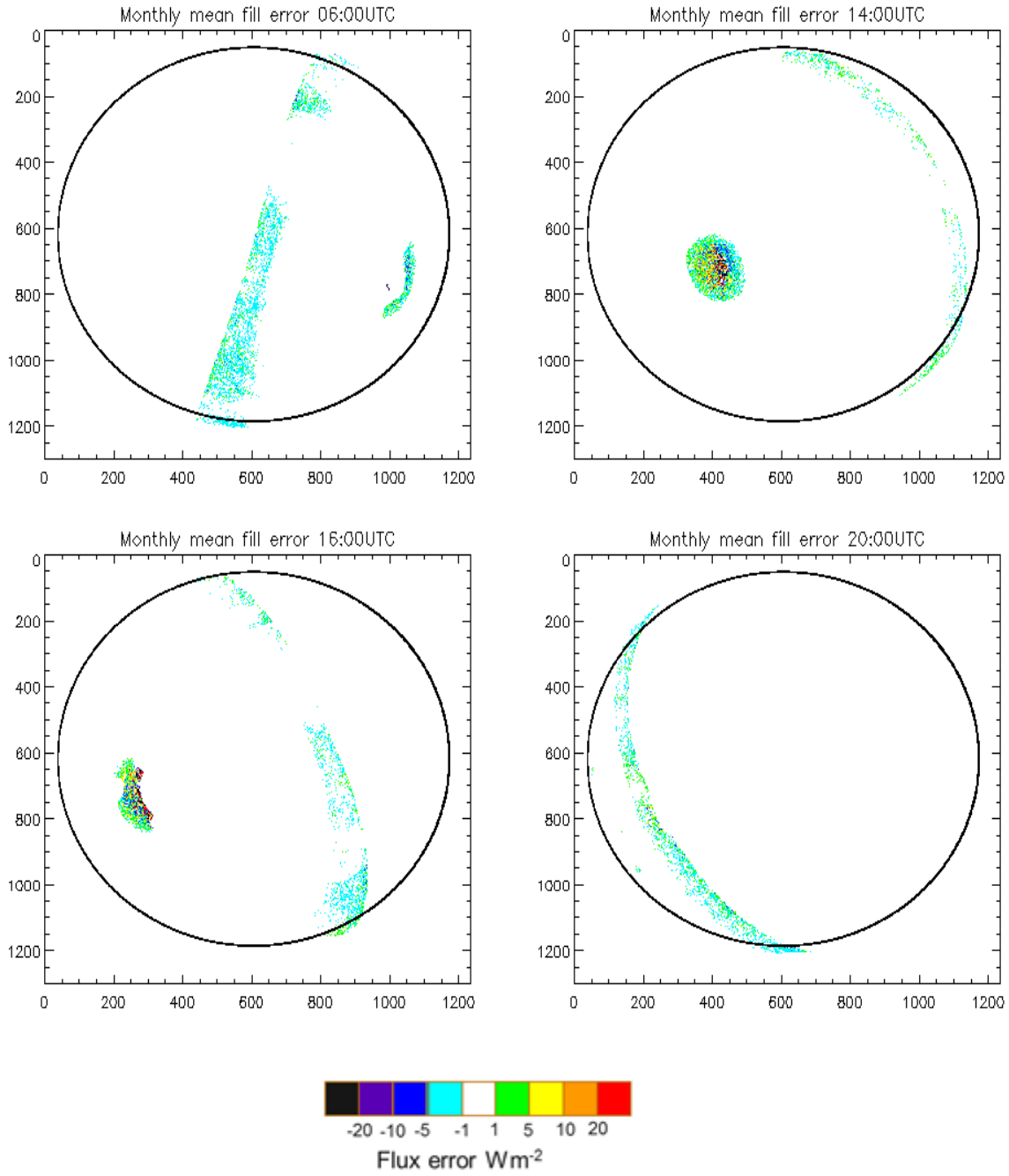

Figure 8: Theoretical bias error in the monthly time-step mean due to scene extrapolation. Above example calculated for GERB 2 November 2004 for the HR 1237x1237 grid point products. Black circle show the limit of the 70° viewing zenith angle.

Figures 9 shows the number of timesteps where the absolute value of the estimated bias in the monthly timestep mean due to scene extrapolation exceeds 10, 6, 2 and 1 Wm^{-2} for the July 2004 example. The glint region is clearly identifiable and the variation of the error magnitude within this region with location / viewing geometry is also apparent.

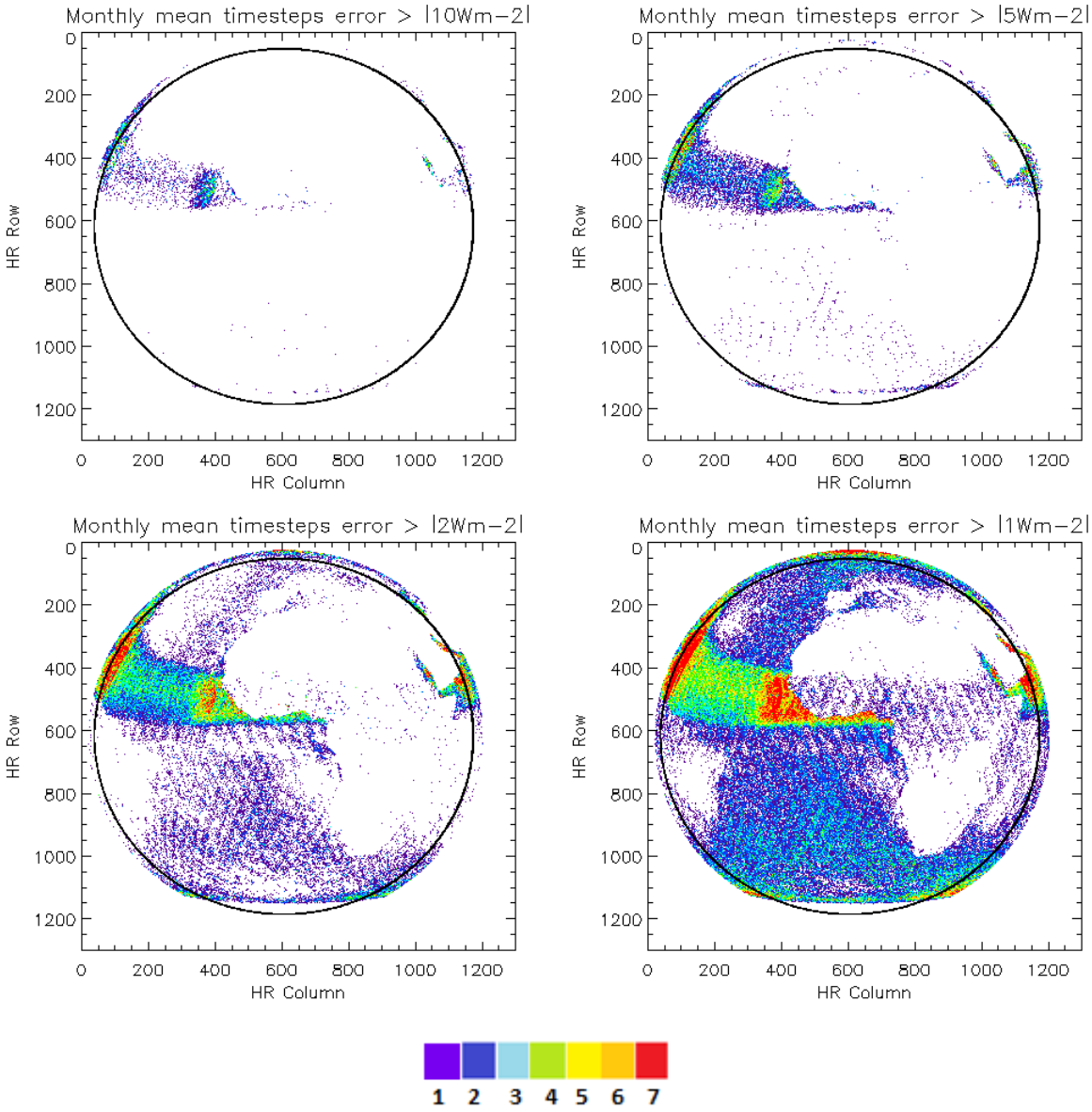

Figure 9: Number of time steps in the monthly time-step mean where the theoretical bias error caused by scene extrapolation exceeds the threshold values shown. Above example calculated for GERB 2 July 2004. Black circle shows the limit of the 70° viewing zenith angle.

Figures 10 shows the bias in the overall monthly mean due to scene extrapolation along with the bias in the monthly timestep mean for the worst affected timestep for both July and November 2004 example cases. The worst timestep error plot is a spatial composite of different timesteps.

It can been seen that in the overall monthly average (top right panel in figure 10) the bias error introduced by filling has a magnitude which is generally less than 5 Wm^{-2} in the geographical region affected by glint for that month and less than 1 Wm^{-2} for the rest of the GERB region. Compare this to error which would result by ignoring the missing data in forming an average (i.e. essentially filling with the average of the reminaing points) this is shown in figure 3 and in the glint region has a magnitude up to 20 Wm^{-2}. Missing data for solar angles higher than 80° has an impact of greater than 1 Wm^{-2} in the monthly average in most of the summer hemisphere, and which exceeds 5 Wm^{-2} at high latitudes in the summer hemisphere.

The errors in the overall monthly mean rarely exceed 5Wm^{-2}. In the monthly timestep mean error in the glint region are mostly in the range ±20Wm^{-2} even for the worst timestep. However a few unfavourable location where the geometry makes the radiance to flux particularly sensitive to scene there are timesteps where the bias does exceed this value. These error should be seen in the context of the complete lack of monthly timestep mean data that would exist in these location at these timesteps in the absence of filling and the error in the monthly mean that would result by not estimating them (see figures 2 and 4).

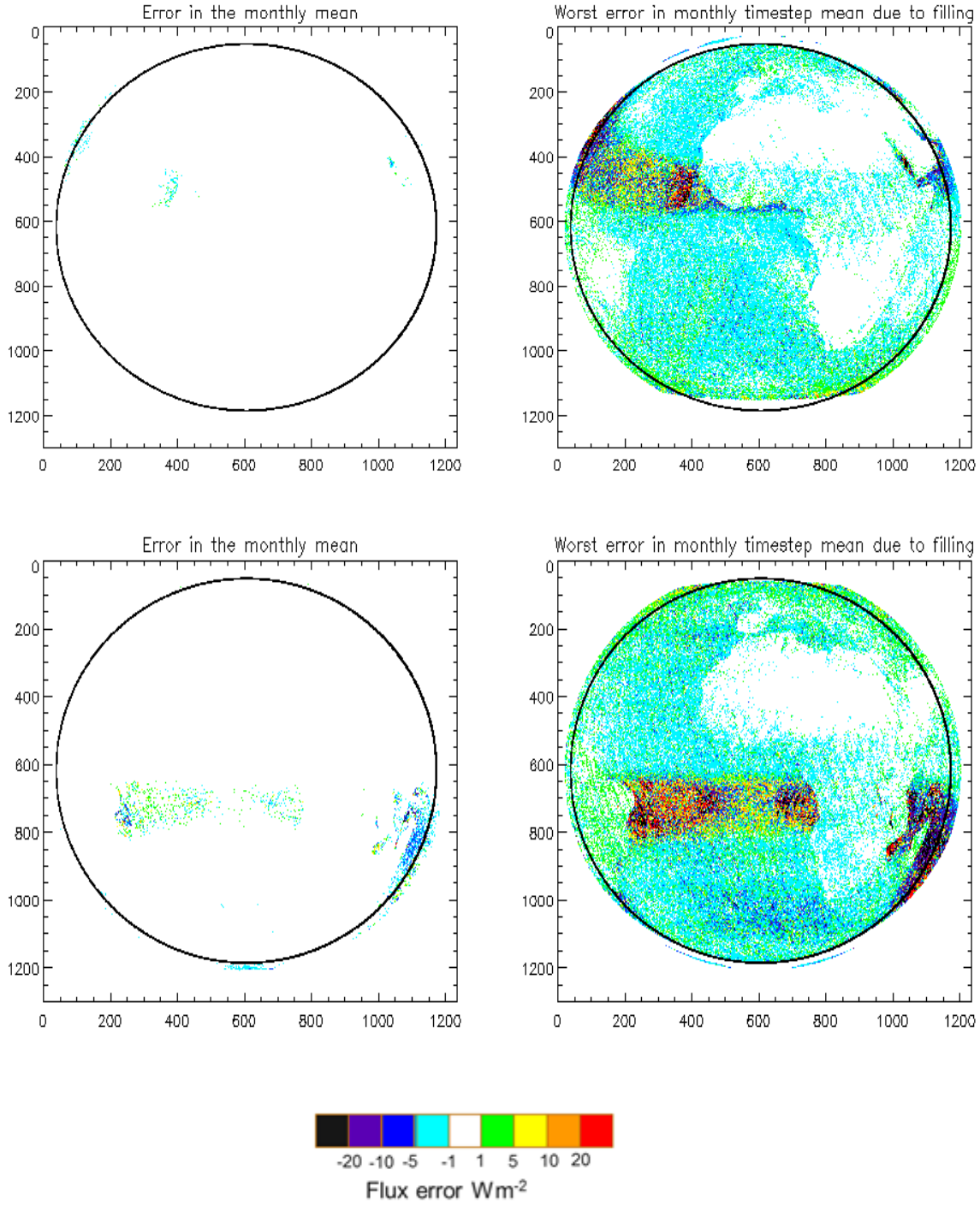

Figure 10. Left: Estimated bias introduced into the monthly mean by expolated scene filling. Right: for each location the bias in the monthly timestep mean for the worst timestep. This composites different timesteps. Top panels are for GERB 2 for July 2004, bottom panels GERB 2 for November 2004. White regions indicate where the bias is < 1 W m-2 in magnitude. The black circle indicate the VZA = 70° limit.

Climatological ocean flux

Fill values 2 and 3 use a GERB climatological ocean flux, specific to that location and month. These fluxes don't use the contemporaneous radiances for the location but are based on clear ocean fluxes observed at different times of day through the whole month adjusted to the observation geometry using the same TRMM models employed in the radiance to flux conversion. This climatological value is not intended to provide a good instantaneous estimate but a low bias monthly mean. The errors associated with it are commensurate with those of radiance to flux conversion in general.

We note that if there is a diurnal cycle in the GERB clear ocean fluxes this would not be reflected in the climatology. This includes any actual diurnal variations in clear ocean flux and spurious diurnal signals due to the how the effect of cloud or aerosol contamination manifests in the fluxes or the effect of biases that result from angle specific errors in the radiance to flux conversion. With the additional screening criteria employed in deriving the clear ocean climatology, no systematic variations with solar zenith are seen in the observed clear ocean fluxes. However it should be borne in mind that the absence of bias variations due to aerosol and cloud contamination in the filled clear ocean points does make their error characteristics different from the clear ocean fluxes at other times of day.

Users should also be aware that a bug in the calculation of monthly climatology introduces a small seasonal bias into the filled clear ocean points. The climatology was derived without accounting for the seasonal variation of the Earth-Sun distance. The resulting bias error for points with fill values 2 and 3 varies systematically with month through the year over the range ±3.4% with peak bias at the solstices. Given the low occurrence of clear sky and the low radiance associated with clear ocean the effect on the monthly average and monthly time step average flux is small. Therefore, the GERB team does not consider user correction required unless users are specifically averaging clear sky ocean points at the monthly time step scale and require accuracy at this level. In these instances, the climatologically filled clear ocean points should be multiplied by d_n^2

Twilight model

A fixed twilight model is applied for SZA in the range 85 to 100° The biases associated with the twilight model is discussed in Kato S., N. G. Loeb, 2003. It should be noted that is applied purely on the basis of SZA and does not account for geographic or seasonal variations in cloud which would have an effect on the twilight flux. Comparisons between integrated GERB radiances for low sun and the CERES twilight model have been made. They indicate there is no significant offset between the GERB and CERES low sun observations.

4. Calibration adjustments to shortwave radiances and fluxes

Several post processing adjustments are discussed below and a combined correction that is recommended that users apply to account for these combined effects is detailed. Further details of the studies which investigated these changes can be found in Parfitt et al. 2016.

Adjustment for GERB 2 shortwave standard correction

After launch and release of the GERB 2 Edition 1 record the output of the shortwave ground source against which it is calibrated was re-examined. This led to an update of its value which implies an adjustment of the GERB 2 shortwave calibration from the value used to process the Edition 1 record. To apply this correction to be Edition 1 data users should multiply all reflected solar radiances and fluxes by 0.976throughout the record. This correction was previously provided to users and where it was applied users were asked to denote the resulting radiances and fluxes as having the SWupdate applied. This correction is now incorporated into the combined correction above and need not be separately applied or noted.

In orbit changes to the shortwave instrument response

The gain of the GERB instrument is updated during operation using observations of the internal black body source. The quartz filter transmission is also monitored in orbit. However the spectral response of the GERB instrument is not monitored after launch and for the Edition 1 products the 'at launch' value is used.

Several sources of evidence suggest that a change to the instrument spectral response, comprising of a loss of response most severe at the shortest wavelengths has taken place during in-orbit operation of both GERB instruments. This is not accounted for in processing the Edition 1 products, and manifests as an apparent reduction over time in the shortwave radiance and hence flux attributed to a given scene which the change being most rapid and severe for the bluest scenes.

The rate of change in the GERB instrument unfiltered reflected solar radiances has now been assessed over the GERB 2 and GERB 1 instrument lifetimes (Parfit et al. 2016), by comparison against CERES FM1 instrument SSF Ed3 reflected solar products. This study found that the ratio of the GERB to CERES reflected solar radiances decreased with time with the rate varying with the spectral properties of the scene and with GERB instrument. Under the assumption that the CERES values are stable over the time period considered (2004 to 2007 for GERB 2 and 2007 to 2012 inclusive for GERB 1) the results imply that the GERB reflected solar radiances recorded for a given scene are decreasing over the record. The rate of change is found to be roughly linear over the operational record but ranges from around 0.4% to 1.9% per year depending on the spectral properties of the scene and the GERB instrument. Figure 7 shows some results from the GERB/CERES comparison studies. The ratio of the CERES filtered to unfiltered radiance (denoted the CERES unfiltering factor) was used to classify the scenes in terms of their spectral properties. The first panel of figure 7 shows the relative proportion of scenes as a function of this classification. The second panel shows the change in the GERB/CERES ratio over the GERB 1 record for scenes in one of the most populous unfiltering factor bins, along with the linear regression line through these points. The third panel shows the gradient of similar regression lines performed over the operational record for each of the unfiltering bins for both GERB 1 and GERB 2.

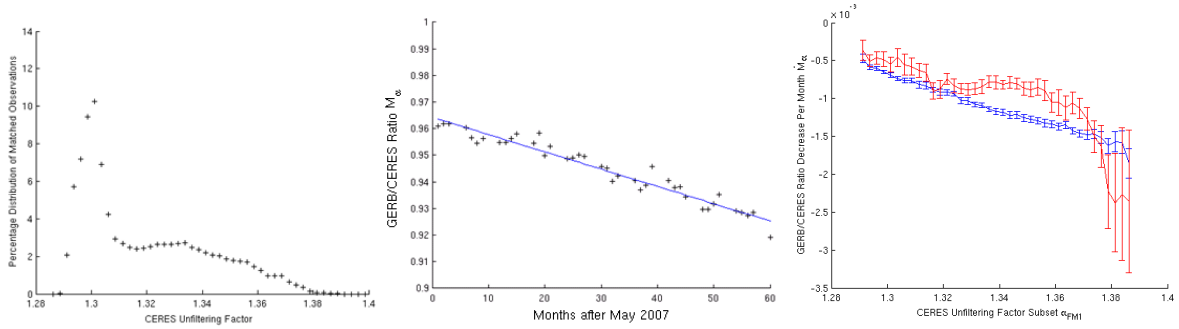

Figure 11. Left: Relative proportion of scenes in each unfiltering factor bin (a measure of the scenes spectral properties). Centre: GERB/CERES ratio for GERB 1 as a function of months after May 2007 (start of the GERB 1 Edition 1 record) for scenes of the most common spectral type (as classified by unfiltering factor). Linear regression line shown in blue. Right: Monthly rate of decrease in the GERB CERES ratio determined as the gradient of linear regression of ratio for GERB 2 (red) and GERB 1 (blue) over their operational record.

Assuming CERES calibration is stable the results imply that averaged over scenes the reflected solar radiation measured by GERB shows a 0.65% annual reduction for GERB 2 and 0.90% annual reduction for GERB 1. Applying such adjustments to the Edition 1 reflected solar radiances and fluxes will provide a mean correction for the in-orbit loss in the GERB shortwave response although residual effects will remain depending on the spectral properties of the scene. The starting point for the GERB 2 record is May 2004 and that of the GERB 1 record May 2007. For GERB 1 users may choose to apply this correction without adjusting for the inter-instrument calibration offset detailed below. This can be

achieved by setting k = 1 for GERB 1 in equation 9, if this approach is used users should denote that they have applied SWaging correction. Please note this approach is only appropriate for GERB 1 data, k must kept to 0.976 for GERB 2 due to the calibration update described above.

Inter-instrument calibration differences

After applying the SWupdate to GERB 2 and correcting for the in-orbit changes due to aging a difference in the reflected solar observations made by GERB-1 and GERB 2 remains. This varies slightly with the spectral properties of the scene but can be approximated by a 5.5% offset between the two instruments across the shortwave. Multiplying the GERB 1 reflected solar radiances and fluxes by 1.055 in addition to the required SWaging correction will provide a reasonable correction for the offset between the two instruments. It is not recommended that users correct calibration offsets without correcting for SWaging.

Recommended user applied combined correction

Adjustment for all the aforementioned effects (GERB 2 standard correction, adjustment for in orbit changes and inter-instrument calibration differences) have been incorporated into the following combined correction. This correction is recommended by the GERB team as a unified correction to apply to the GERB Edition 1 reflected solar (SW) radiances and fluxes SW(ED1) as follows

$$SW(ED1\ SW\ comb\ corr) = k\left[\frac{SW(ED1)}{1-\varepsilon t}\right] \qquad [9]$$

where t is the time in fractional years since the start of the operational record, i.e.1st May 2004 for GERB 2 and 1st May 2007 for GERB 1.

The correction coefficients vary with GERB instrument and the time period of the data.

For GERB 1: k = 1.055, ε = 0.00824

For GERB 2 k = 0.976, ε = 0.00655

This correction should be applied to both filled and unfilled fluxes when SZA > 85° but not to points flagged as filled with the twilight model. Strictly speaking twilight model fluxes should be uncorrected in GERB 1 and multiplied by 0.976 for GERB 2. However, as noted earlier, the additional error by leaving them completely uncorrected in both datasets is small compared to the filling biases and other error sources. Thus for simplicity users are advised to leave all twilight model fluxes unaltered.

All Edition 1 data so corrected by users should be denoted as having the ED 1 SW combined correction (SWcombcorr).

5. References

N. Clerbaux, S. Dewitte, C. Bertrand, D. Caprion, B. De Paepe, L. Gonzalez, A. Ipe, J.E. Russell and H. Brindley (2008a): Unfiltering of the Geostationary Earth Radiation Budget (GERB) Data. Part I: Shortwave Radiation, *Journal of Atmospheric and Oceanic Technology*, **25(7)**, 1087-1105.

N. Clerbaux, S. Dewitte, C. Bertrand, D. Caprion, B. De Paepe, L. Gonzalez, A. Ipe and J.E. Russell (2008b): Unfiltering of the Geostationary Earth Radiation Budget (GERB) Data. Part II: Longwave Radiation, *Journal of Atmospheric and Oceanic Technology*, **25(7)**, 1106-1117.

S. Dewitte, L. Gonzalez, N. Clerbaux, A. Ipe, C. Bertrand, B. De Paepe (2008): The Geostationary Earth Radiation Budget Edition 1 data processing algorithms, *Advances in Space Research*, **41(11)**, 1906-1913.

Harries JE, Russell JE, Hanafin JA, Brindley H, Futyan J, Rufus J, Kellock S, Matthews G, Wrigley R, Last A, Mueller J, Mossavati R, Ashmall J, Sawyer E, Parker D, Caldwell M, Allan PM, Smith A, Bates MJ, Coan B, Stewart BC, Lepine DR, Cornwall LA, Corney DR, Ricketts MJ, Drummond D, Smart D, Cutler R, Dewitte S, Clerbaux N, Gonzalez L, Ipe A, Bertrand C, Joukoff A, Crommelynck D, Nelms N, Llewellyn-Jones DT, Butcher G, Smith GL, Szewczyk ZP, Mlynczak PE, Slingo A, Allan RP, Ringer MA et al., 2005, The geostationary Earth Radiation Budget Project, *BULLETIN OF THE AMERICAN METEOROLOGICAL SOCIETY*, Vol: 86, Pages: 945-+, ISSN: 0003-0007

Kato S., N. G. Loeb, 2003. Twilight Irradiance reflected by the Earth estimated from Clouds and the Earth's Radiant Energy System (CERES) Measurements. J. Clim., 16: 2646-2650.

Loeb N. G., K. Loukachine K, N. Manalo-Smith, B. A. Wielicki, D. F. Young, 2003. Angular distribution models for top-of-atmosphere radiative flux estimation from the Clouds and the Earth's Radiant Energy System instrument on the Tropical Rainfall Measuring Mission satellite. Part II: Validation. J Applied Meteorology 42 (12): December 1748-1769

Parfitt R, Russell JE, Bantges R, Clerbaux N, Brindley He t al., 2016, A study of the time evolution of GERB shortwave calibration by comparison with CERES Edition-3A data, *REMOTE SENSING OF ENVIRONMENT*, Vol: 186, Pages: 416-427, ISSN: 0034-4257

6. Further information and user documents

The following applicable documents contain further relevant details and are available from the GERB edition data distribution archives:

Quality Summary: GERB level 2 Edition 1: Essential information for users of the GERB products, required reading.

Product processing and accuracy summary: [this document] Updated document describing the GERB processing and providing theoretical accuracy statements of the data fields. Recommended reading for all users of the GERB data. Includes sections of the aging and the treatment of fill fields of relevance to the latest release.

Level 2 ARG Edition 1 release validation report: Validation studies completed at the time of the ARG edition 1 release. Includes comparison with older CERES products (CERES SSF Ed 2). Incorporates the required user applied ground calibration update for GERB 2 comparisons, but does not include the latest recommended user revisions that unify and stabilise the GERB records.

Level 2 HR Edition 1 release validation supplement: Latest validation for the filled HR and BARG Edition 1 release. Comparisons with later versions of CERES data (CERES SSF Ed 3 and Ed 4). Consideration of the filled data and the latest user revisions for aging and unification of the record.

RMIB GERB products user guide: automatically generated document detailing every field contained in all the GERB level 2 products.

Quality Summary for GERB Edition 1 L1.5 NANRG and GEO products: NANRG release quality and validation document. As the level 1.5 products form the basis of the level 2, users of the level 2 may find the information useful background.

GGSPS products user guide: provides background information on product definitions relevant to all products and details of the parameters contained in the level 1.5 GERB data